

## Niobium Sputter Coated Stainless Steel as a Bipolar Plate Material for Polymer Electrolyte Membrane Fuel Cell Stacks

Jun-Ho Kim<sup>1</sup>, Sun-Kwang Kim<sup>1</sup>, Yong-Zoo You<sup>1</sup>, Dae-Il Kim<sup>1</sup>, Sung-Tae Hong<sup>2,\*</sup>,  
Ho-Cheol Suh<sup>3</sup>, K. Scott Weil<sup>4</sup>

<sup>1</sup> School of material science and engineering, University of Ulsan, P.O. Box 680-749, Ulsan, South Korea

<sup>2</sup> School of mechanical engineering, University of Ulsan, P.O. Box 680-749, Ulsan, South Korea

<sup>3</sup> Sejong Industrial Company LTD., P.O. Box 683-360, Ulsan, South Korea

<sup>4</sup> Pacific Northwest National Laboratory, Richland, WA, 99352, USA

\*E-mail: [sthong@ulsan.ac.kr](mailto:sthong@ulsan.ac.kr)

*Received:* 1 August 2011 / *Accepted:* 19 August 2011 / *Published:* 1 September 2011

---

Niobium (Nb) sputter coated 316L stainless steel (SS) is investigated as an alternative to a previously developed Nb clad 304L SS material for use in a bipolar plate component of a polymer electrolyte membrane fuel cell (PEMFC) stack. The electrochemical properties of the Nb sputter coated 316L SS are evaluated via static corrosion and interfacial contact resistance testing and through potentiodynamic and potentiostatic measurements conducted under half-cell environments of a standard PEMFC stack. The experimental results show that the electrochemical properties of the sputtered Nb coatings are quite viable for the PEMFC bipolar plate application, while the thickness of the sputtered Nb coating is substantially thinner than that of the roll clad Nb coating.

---

**Keywords:** niobium, sputtering, stainless steel, bipolar plate, polymer electrolyte membrane fuel cell.

### 1. INTRODUCTION

The use of a polymer electrolyte membrane fuel cell (PEMFC) system as a primary power source for automotive transportation continues to be a potentially viable alternative to the traditional internal combustion engine. This is due to the high specific power, low operating temperature (~80°C), and high energy conversion efficiency that PEMFC stacks offer [1]. However, although various automakers have made significant progress toward bringing PEMFC vehicles closer to commercial reality, there remain several major technical hurdles to overcome, including [1-4]:

- Reducing the projected high-volume manufacturing cost of PEMFC stacks.

- Extending the useful operating lifetime of the PEMFC stack to match that of the vehicle.
- Reducing the size and weight of the overall PEMFC system by 2–3 times the current average values.

Although the primary factor in projected stack cost is the amount (and spot price) of the platinum (Pt) catalyst employed in the anode and cathode layers, the second-most expensive stack component often is the bipolar plate [3]. By far the bulkiest and heaviest repeat component in each cell, the bipolar plate acts as an electrical interconnection between adjacent cells, separately distributes fuel and oxidant to the gas diffusion layers while inhibiting mixing of the two gas streams, promotes water and heat removal, and provides mechanical support for the stack [4].

Currently there are two leading classes of materials being developed for the bipolar plate component: carbon- or graphite-based composites and metal alloys. The former generally offer acceptable bulk electrical conductance, excellent corrosion resistance in the acidic environment of the stack, and minimal effect on the degradation of stack power output. Current development efforts on carbon-based composite bipolar plates are focused on reducing the cost of manufacture and improving their mechanical characteristics (such as flexure strength and toughness), imperviousness to through-thickness mass transport (namely fuel, oxidant, and/or water vapor), and thermal conductivity, while reducing plate thickness to a sub-millimeter range [4,5].

By comparison, low-cost/high-volume manufacture of metallic bipolar plates via stamping or sheet embossing is well understood. The metallic bipolar plates, which can be fabricated in very thin form (<150  $\mu\text{m}$ ), are intrinsically impermeable to through-thickness vapor transport, and exhibit excellent thermal conduction properties and mechanical robustness. The critical concern with metallic bipolar plates (such as iron-, nickel-, titanium-, and aluminum-based plates) is surface corrosion, which leads to a release of metal ions that can contaminate the electrolyte membrane and poison the electrode catalysts [1,6,7]. Also, the formation of a passivating oxide or oxyhydroxide layer on the surface of the metal increases the contact resistance between the bipolar plate and the adjacent carbon-based gas diffusion layer (GDL), often by many orders of magnitude. This limits the amount of power that can be generated by the stack and acts as a source of resistive heating (in addition to that normally generated by the anode and cathode reactions) that must be removed during stack operation.

Scott et al. [8,9] have recently shown that commercially pure niobium (cp-Nb) exhibits sufficient long-term corrosion resistance and surface conductance to meet generally accepted technical targets for the PEMFC bipolar plate application. However cp-Nb is over an order magnitude more expensive on a per kilogram basis than the commonly employed stainless steel alloys. Thus a metal cladding concept was considered. A thin 12.5  $\mu\text{m}$  layer of cp-Nb was clad to a thicker (125  $\mu\text{m}$ ) 304L stainless steel (SS) sheet via commercial roll bonding practice [9]. Results from linear voltammetry and potentiostatic testing conducted under aggressive conditions demonstrate that the material is electrochemically viable, exhibiting a passivating behavior at standard anode and cathode operating potentials, which is comparable to that of non-corrosive noble metals such as Pt. Measurements of the contact resistance between a representative Toray<sup>TM</sup> GDL paper and the Nb side of the clad sheet in the as-received or passivated conditions were comparable to previously reported values for graphite bipolar plate materials [9].

A preliminary characterization of the mechanical properties of the clad material in the as-rolled and post-roll annealed conditions indicated that annealing may be required to restore sufficient ductility for the subsequent blanking, stamping, and bending operations needed to form the final bipolar plate configuration [10]. However, the annealing step employed in that study (a high vacuum annealing at 982°C for 900 sec) generated an intermetallic phase at the interface between the cladding and substrate layers. According to Hong et al. [11], the formation and composition of the phase, which may cause failure of the annealed Nb clad 304L SS under high strain conditions [10], are strongly affected by the annealing temperature and time. To avoid the need for annealing and thereby mitigate the subsequent formation of a brittle interfacial layer between the niobium and underlying stainless steel, an alternative Nb sputter coating approach was suggested [12]. Reported here are results from electrochemical testing of Nb sputter coated 316L SS under a typical PEMFC operating environment.

## 2. EXPERIMENTAL SET-UP

Disc-shaped specimens measuring 22 mm in diameter and 6 mm in thickness were fabricated from austenitic 316L SS. The specimens were ground and polished to a RMS finish of 15–20 nm. The specimens were then ultrasonically degreased in acetone and methanol, followed by a distilled water rinse and air drying prior to sputter coating. 1.5  $\mu\text{m}$  thick Nb films were deposited on the stainless steel specimens by DC reactive magnetron sputtering using the process parameters listed in Table 1. A 99.95% purity Nb sputtering target measuring 76 mm in diameter and 6.4 mm in thickness was employed.

**Table 1.** Process parameters for DC magnetron sputtering

Target material	Nb, (99.95% purity)
Substrates	316L SS
Substrate temperature	Room temperature
Target power	300 W
Argon pressure	3 mTorr
Target to substrate distance	60 mm

Scanning electron microscope (SEM) analysis was conducted to examine the microstructure and thickness of the deposited Nb film using a JEOL JSM-5900LV system. Immersion testing of all the Nb-sputtered specimens were carried out according to ASTM G31-72 [13] at 80°C in static 1M H<sub>2</sub>SO<sub>4</sub> containing 2ppm HF, an aqueous solution equivalent to the most aggressive pH (no current) condition under which the bipolar plate would be exposed in the stack [9,14]. Coupons were removed after 50, 100, 200, and 300 hrs of exposure, dried and weighed, and compared with their initial pre-exposure weight to determine the amount of metal loss that occurred. Also, the effluent to which each sample was exposed was analyzed by inductively coupled plasma mass spectrometry (ICP-MS;

Agilent 4500) to determine the amount of Nb and iron (Fe) that dissolved in the solution over the period of exposure.

Interfacial contact resistance (ICR) between the Nb sputter coated specimen and carbon paper (Toray, Inc., TGP-H090), a typical gas diffusion layer (GDL), was measured as a function of compressive pressure applied to the carbon paper/sputtered specimen/carbon paper stack using a technique similar to the method described in Mishra et al. [15], as schematically shown in Figure 1.

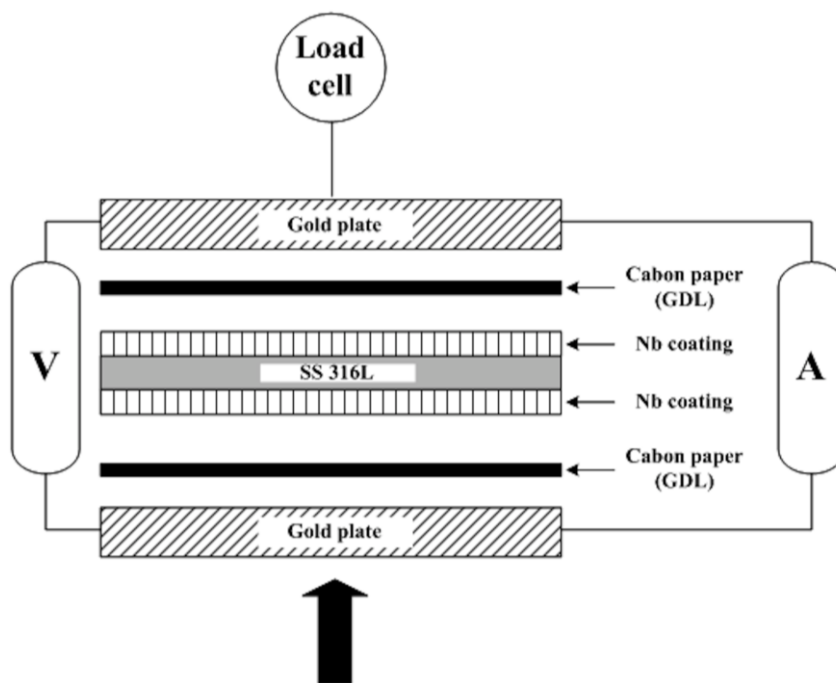


**Figure 1.** A schematic of an ICR measurement set-up

For the ICR measurements, both sides of each specimen were coated with Nb. An electrical current of 1 A was applied from one side to the other side via leads using a Hewlett-Packard 3263A DC power source. The resulting voltage drop was measured as a function of clamping pressure from 0.5 to 2.5 MPa through a separate set of leads using an Agilent 34420A multimeter, thereby establishing a four point measurement that eliminates lead resistance. The measured ICRs of the Nb-sputtered SS were compared those of the Nb clad SS [9,10].

The electrochemical properties of the Nb sputter coated SS specimens were measured at 80°C in 1M H<sub>2</sub>SO<sub>4</sub> containing 2 ppm HF. A standard three-electrode system (Gamry, DC105 corrosion measurement system) was used in polarization testing. A platinum plate, a Ag/AgCl electrode, and the specimen were used as the counter, reference, and working electrodes, respectively. During testing, air or H<sub>2</sub> gas was sparged through the H<sub>2</sub>SO<sub>4</sub> solution to respectively simulate the PEMFC cathode or anode environment. The specimen was stabilized in the solution at open circuit for 30 min prior to conducting the measurement. The potentiodynamic polarization curve was scanned from -1.5 V to 2 V at a rate of 5 mV/sec. Potentiostatic experiments were also conducted to gage the performance of the coated specimen under prototypic PEMFC operating conditions. After allowing the specimen to

stabilize in the solution, a potential was applied and the resulting current/time curves were recorded for 3 hr. Cathodic testing was conducted in sparged air at a potential of +0.6 V, while anodic testing was conducted in sparged hydrogen at -0.1 V.

### 3. RESULTS

#### 3.1. Microstructures of Nb sputtering layer

Results from SEM analysis indicate that the sputtered Nb layer exhibits a microstructure that is quite different from that of the clad Nb layer [10], as shown in Figures 2(a) and (b). A columnar grain structure is observed in the cross-sectional micrograph of the sputtered sample in Figures 2(a), a microstructure that is typical for relatively thick sputter-coated specimens [16]. Note that the insert in Figure 2(b) shows a cross-sectional micrograph with a low magnification including clad Nb layer and SS substrate.

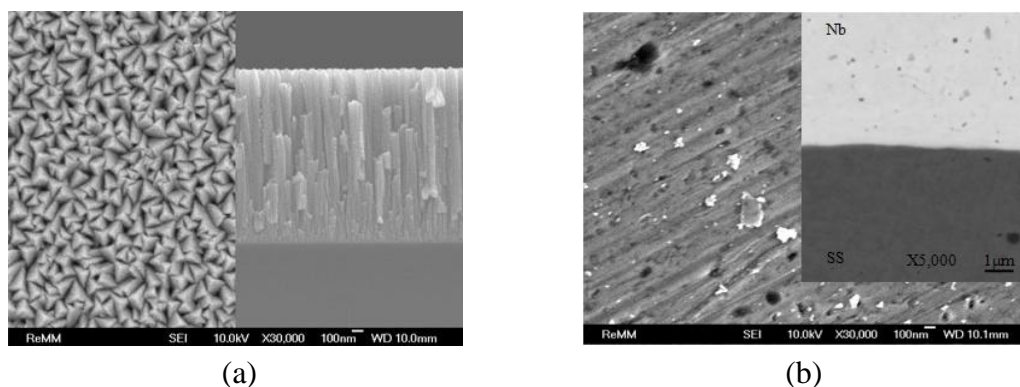


**Figure 2.** Planar and cross-sectional SEM images of the sputtered Nb film and (b) a cross-sectional SEM image of the Nb clad layer of a 10%Nb-clad 304L SS material in the as rolled condition [10]

#### 3.2. Exposure testing

Shown in Table 2 are the results from the immersion testing. Weight measurements taken directly on the specimens before and after exposure indicate that the specimens experienced essentially no change in weight within  $\pm 0.01\%$  of the original weight, which suggests that the Nb-sputter coated layers are quite resistant to corrosion under the given condition. These results are validated by the ICP-MS measurements of the amount of Nb dissolved in the corresponding effluent solutions, provided in column 3 of Table 2. Also listed in Table 2 are the results of the ICP-MS measurements of the amount of Fe eluted from the underlying SS substrate, presumably through pinhole defects in the coating. At a level of approximately 1 ppm, the amount of dissolved iron is quite small, indicating that the Nb sputter layer effectively protects the stainless steel substrate. It is anticipated that even this small

pinhole effect can be further reduced by optimizing the sputtering process to produce a Nb layer with fewer defects.

**Table 2.** Results of immersion testing at 80°C in 1 M H<sub>2</sub>SO<sub>4</sub> with 2 ppm HF

Parameters	Unit	Results			
		50 hrs	100 hrs	200 hrs	300 hrs
Fe	PPM	0.4066	0.8851	1.0017	1.3506
		1			
Nb	PPM	0.0137	0.0775	0.3996	1.4339
		2			
Wt loss	%	0	0	0	0

### 3.3. Interfacial Contact Resistance (ICR)

Measurements of the area-specific ICR between the as-prepared Nb sputter coated specimen and a representative GDL carbon paper are shown in Figure 3 as a function of the clamping pressure. The contact resistance decreases dramatically with increasing clamping pressure, a trend that is typically observed in these types of measurements for metal bipolar plate candidate materials [17-20]. Measurements of the area specific ICR between the Nb sputter coated specimen that underwent static exposure testing and a representative GDL carbon paper are also shown in Figure 3 as a function of the clamping pressure.

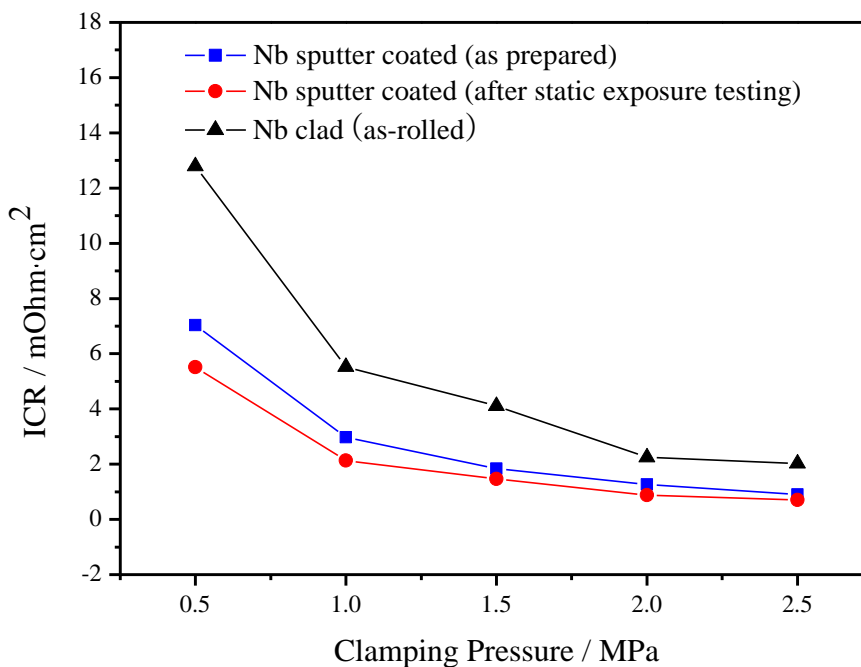
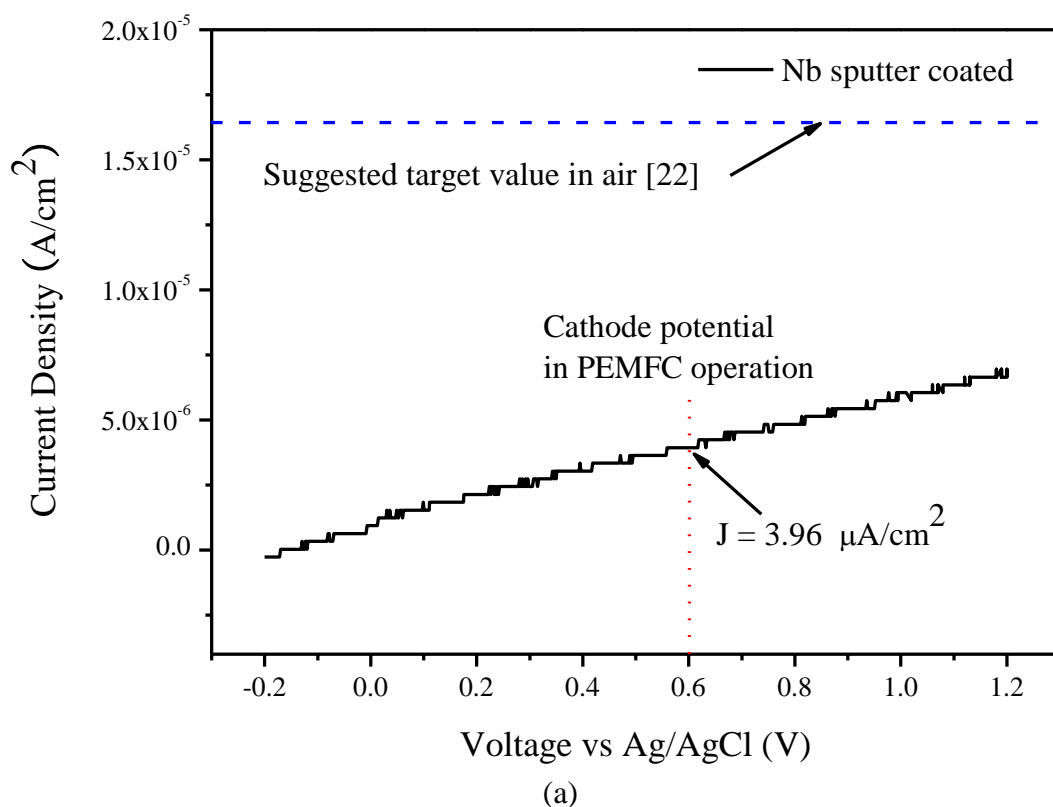


**Figure 3.** Results of ICR measurement as a function of clamping pressure.

Comparison of these results indicate that the corrosion passivation layer that forms on the niobium surface exhibits little effect on the contact resistance between the Nb sputter coated bipolar plate material and the carbon paper. As a reference, the pressure dependent ICR between the carbon paper and an as-rolled Nb clad specimen (12 μm thick Nb layer roll bonded to a 0.24 mm thick 304L SS substrate) is also shown in Figure 3. The ICR curve for the Nb sputter coated specimen is significantly lower than that of the Nb clad specimen at all levels of clamping pressure. It is speculated that this may be due to the smoother surface finish of the sputter coated specimen vis-à-vis the roll clad material.

### 3.4. The corrosion properties

Shown in Figures 4(a) and (b) are the polarization curves for the Nb sputter coated 316L SS specimen in 1 M H<sub>2</sub>SO<sub>4</sub> + 2 ppm HF at 80°C under sparged air and H<sub>2</sub>, respectively. For reference, the typical operating potentials at each electrode (i.e. a cathode potential of 0.6 V and an anode potential -0.1 V) are marked in the respective figures. The current densities measured in the Nb sputter coated specimens at 0.6 V (sparged air) and -0.1 V (sparged H<sub>2</sub>) were respectively 3.96 μA/cm<sup>2</sup> and -17.7 μA/cm<sup>2</sup>. Even though each value, which represents a corrosion resistance under the given half cell operating environment, is lower than the value previously observed in the Nb clad 304L SS [9], the direct comparison of the corrosion resistances of the Nb sputter coated 316L and the Nb clad 304L should be conducted with a care since different substrates were used [21].



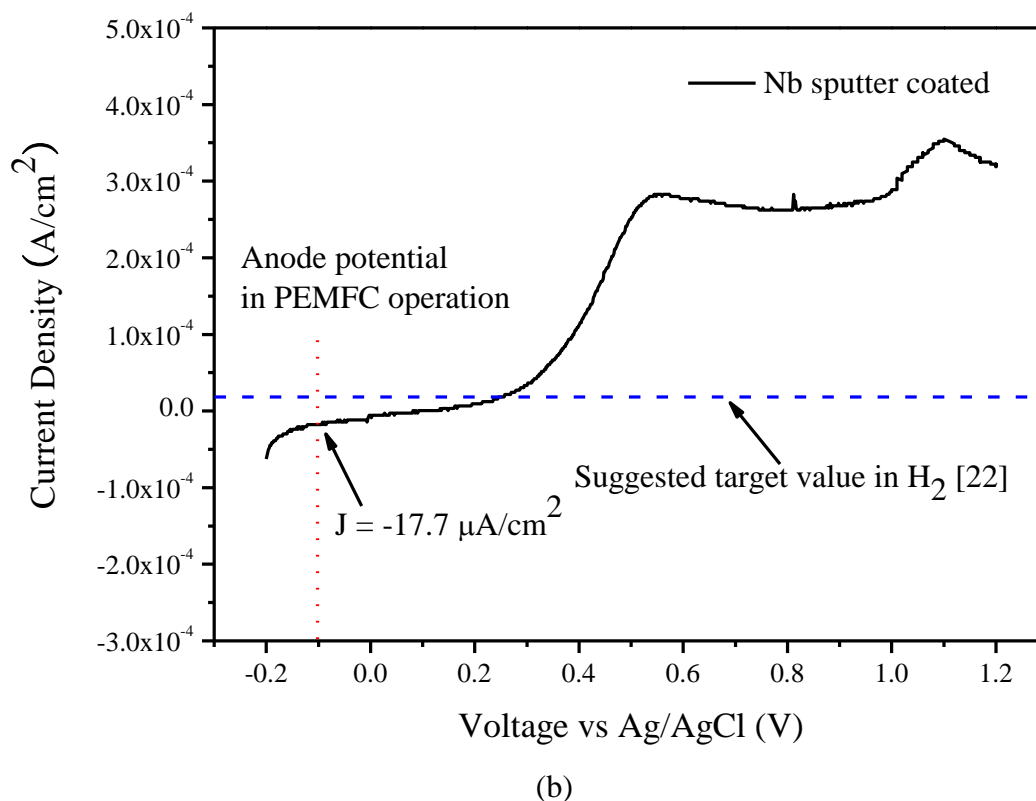


**Figure 4.** Potentiodynamic curves of the Nb sputter coated specimens under: (a) a cathodic and (b) an anodic environment

Instead, the thing should be noted is that these values are lower than the generally recommended upper limits for acceptable stack operation,  $16 \mu\text{A}/\text{cm}^2$  [22], while the thickness of the Nb coating of the Nb sputter coated specimen was significantly thinner than that of the Nb clad specimen. In general, the minimum thickness of Nb coating in the cladding concept is decided by the limitation of the conventional roll-cladding process.

Also note that the current densities measured in the bare 316L SS at 0.6 V (sparged air) and -0.1 V (sparged  $\text{H}_2$ ) were respectively  $40.67 \mu\text{A}/\text{cm}^2$  and  $75.1 \mu\text{A}/\text{cm}^2$ , both of which are significantly higher than the recommended upper limits for acceptable stack operation [22]. Actually, the bare 316L SS quickly showed a serious general corrosion including a porous layer on the surface during the following potentiostatic testing. It is apparent that the bare 316L SS is not suitable for a bipolar plate material of PEMFC stacks.

Results from potentiostatic testing confirm the corrosion resistance of the Nb sputter coated material in each half-cell environment, as shown in Figures 5(a) and (b). Both transient current density curves decay quickly reaching stable values,  $2.71 \mu\text{A}/\text{cm}^2$  under the cathodic condition and  $-84.0 \mu\text{A}/\text{cm}^2$  under the anodic condition, both of which are well below the generally recommended upper limit values [22].



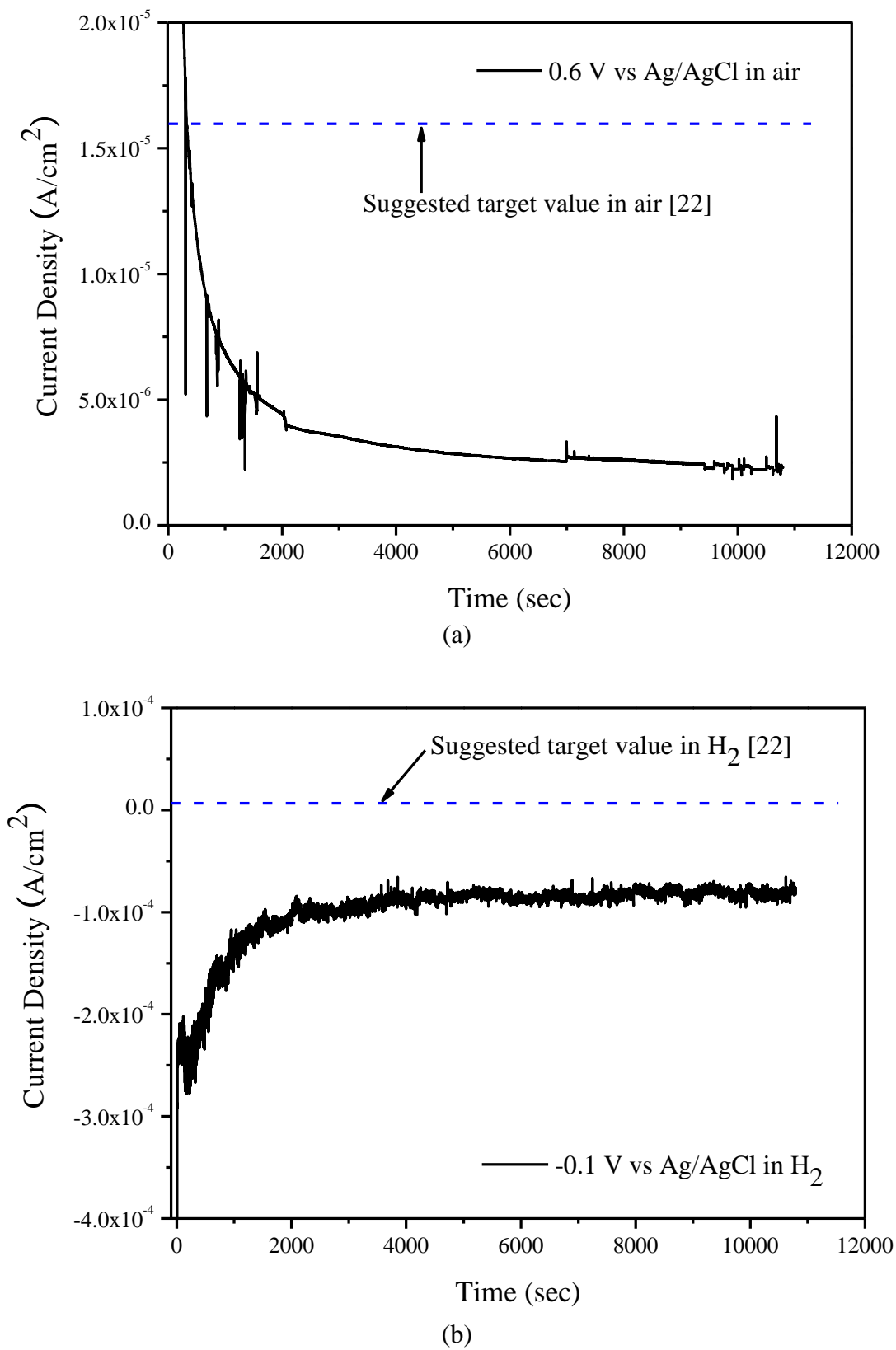


**Figure 5.** Potentiostatic curves of the Nb sputter coated specimens under: (a) a cathodic and (b) an anodic environment

Note that the both stabilized current densities for anodic and cathodic conditions were calculated by averaging the current density from 4000 to 9000 sec. The decay and eventual stabilization in current density are related to passivation taking place on the surface of the Nb coating. Planar images of the sputter coated specimens prior to and after potentiostatic testing in purged H<sub>2</sub>, shown respectively in the SEM micrographs of Figures 6(a) and (b), indicate essentially no change in the surface morphology of the Nb coating due to electrochemical testing.

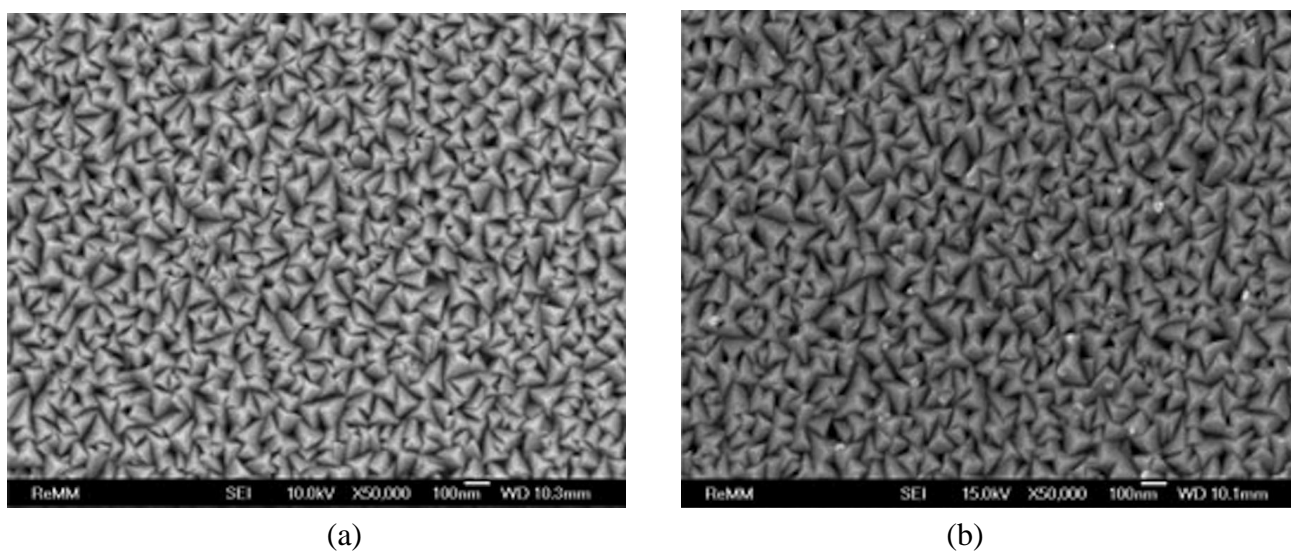


**Figure 6.** Planar SEM images obtained on Nb sputter coated specimens: (a) prior to and (b) after the potentiostatic test in purged H<sub>2</sub>

### 3.5. Discussion of process viability: Nb sputtering vs. cladding

As presented above, the electrochemical properties of the Nb sputtered coatings are quite viable for the PEMFC bipolar plate application. Also, sputtering offers the potential to decrease the Nb layer thickness to sub-micron scale as a means of reducing raw material cost in the finished plate. By comparison, the minimum thickness achievable by roll bonding is estimated to be between 6–12  $\mu\text{m}$  for the Nb clad coatings, which electrochemical properties are also viable for the PEMFC bipolar plate application [9].

A thorough economic analysis would need to be conducted to more carefully compare the overall cost and nominal production rate anticipated for each process. However, recent works by Hong et al. [10,11] raise additional considerations for the clad metal concept: (1) the as-rolled product probably needs to be annealed prior to secondary metal forming to eliminate excessive work hardening in each layer that was induced by the roll cladding process and (2) current data suggest that this annealing heat treatment will likely lead to the formation of an intermetallic phase at the interface between the substrate and coating material.

This interfacial phase can lead to failure of the composite under high-strain forming conditions [10]. Thus the need for annealing in the clad material may add an additional constraint in the design of the flow channels for this type of composite bipolar plate.

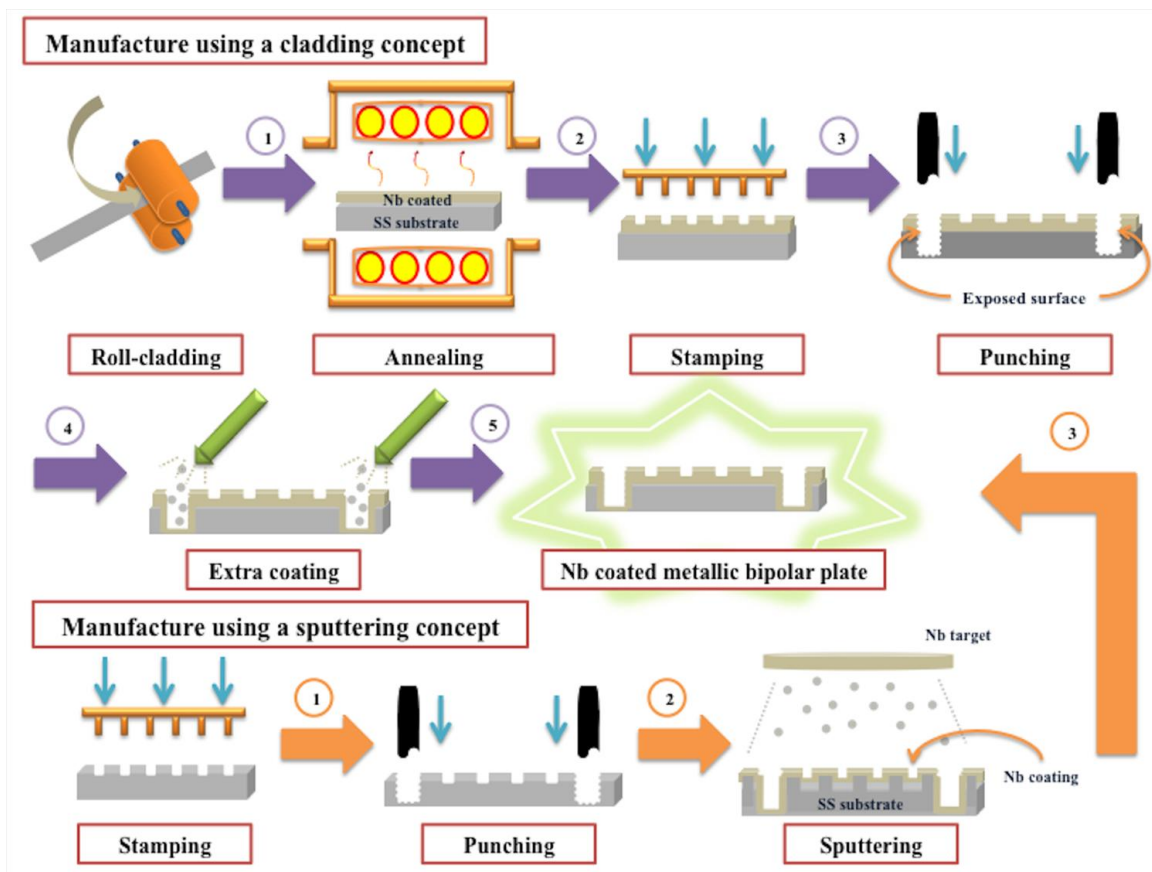


**Figure 7.** A comparison of manufacturing processes of metallic bipolar plates using a sputtering concept and a cladding concept

As noted in Figure 7, clad metal bipolar plates would also likely need a secondary coating or alternative method of protecting the unclad edges intrinsic to internal flow-through holes in the plate design. The holes allow for liquid and gas transport from one cell to the next in the stack and would be formed via a punching or blanking process. By comparison, sputter coating can be applied as a final process step in the manufacture of metallic bipolar plates. This avoids potential issues with annealing, blanking, punching, and forming of the underlying sheet metal, all of which would take place prior to the final application of the thin protective Nb layer.

#### 4. CONCLUSION

Nb sputter coated SS was evaluated as a potential PEMFC bipolar plate material. Results from exposure testing and corresponding ICP-MS measurements of acid bath effluent demonstrated no gross

corrosion in the specimens, indicating that the sputtered Nb layer provides sufficient corrosion resistance for the entire material. ICR measurements of the Nb sputter coated specimen show that the material offers pressure-dependent contact resistance, which meets the current U.S. Department of Energy target for the bipolar plate component at all of the clamping pressures evaluated, with a prototypic GDL material (Toray carbon paper) even after undergoing passivation via exposure testing. Potentiodynamic testing employed in the electrochemical property measurements, using either sparged air or H<sub>2</sub>, indicated very low passivation currents for both the cathodic and anodic half-cell reactions. The results from subsequent potentiostatic testing confirm the corrosion resistance of the Nb sputtered coating under prototypic half-cell operation; again, the measured current densities meet the desired performance metric for this test. These experimental results suggest that the electrochemical properties of the Nb sputter coated 316L SS are quite viable for the PEMFC bipolar plate application at a Nb layer thickness that is only ~10% of the cladding, which thickness limits generally come from the characteristic of the conventional roll-cladding process. Also, Nb sputtering may hold several process advantages over the clad metal concept, including: (1) mitigation of an annealing step in the Nb/SS material that can induce the formation of a deleterious intermetallic interfacial phase, (2) application of a thinner protective (i.e. potentially less expensive) Nb layer, and (3) an opportunity to apply the Nb after all sheet metal processing operations (e.g. annealing, stamping, blanking, etc.) are complete, which minimizes the potential for forming a high concentration of process defects within the protective coating.

#### ACKNOWLEDGEMENT

This work was supported by the development program of local science park funded by the ULSAN Metropolitan City and the MEST (Ministry of Education, Science and Technology), South Korea. The Pacific Northwest National Laboratory is operated by Battelle Memorial Institute for the United States Department of Energy under Contract DE-AC06-76RLO 1830.

#### References

1. P. Adcock, A. Kells, and C. Jackson, EET-2008 European Ele-Drive Conference Proceedings, International Advanced Mobility Forum, Geneva, Switzerland, March 11, 2008.
2. N. de las Heras, E.P.L. Roberts, R. Langton, and D.R. Hodgson, *Energy & Env. Sci.* 2 (2009) 206-214.
3. U.S. Department of Energy, Hydrogen, Fuel Cells & Infrastructure Technologies Program Multi-Year Research, Development and Demonstration Plan (2005 – 2015), available at <http://www.eere.energy.gov/hydrogenandfuelcells/mypp/>, last accessed on March 1, 2010.
4. A.Hermann, T. Chaudhuri, P. Spagnol, *Int. J. Hydrogen Energy* 30 (2005) 1297-1302.
5. G. Rinn, S. Bornbaum, *Ceram. Forum Int.* 82 (2005) E33-E36.
6. R. Hornung, G. Kappelt, *J. Power Sources* 72 (1998) 20-21.
7. J.A. Sawicki, T. Tyliczszak, F.E. Wagner, J.H. Rolston, A.P. Hitchcock, D.E. Clegg, *Phys. B* 158 (1989) 203-205.
8. K.S. Weil, J.Y. Kim, G.G. Xia, Z.G. Yang, Clad metal material for PEMFC bipolar plates, U. S. Patent Office, in review.
9. K.S. Weil, G. Xia, Z.G. Yang, J.Y. Kim, *Int. J. Hydrogen Energy* 32 (2007) 3724-3733.
10. S.-T. Hong, K.S. Weil, *J. Power Sources* 168 (2007) 408-417.

11. S.-T. Hong, K.S. Weil, I.-T. Bae, J.P. Choi, J. Pan, *J. Power Sources* 195 (2010) 2592-2598.
12. S.-T. Hong, Y.-Z. You, J.-H. Kim, Bipolar plate for polymer electrolyte membrane fuel cell and the methods for fabricating the same, R.O.K Patent Office, in review.
13. ASTM, Standard Practice for Laboratory Immersion Corrosion Testing of Metals. ASTM G31-72. Philadelphia: ASTM; 1995.
14. D. Chu, R. Jiang. *J. Power Sources* 80(1-2) (1999) 226-234.
15. V. Mishra, F. Yang, R. Pitchumani, *J. Fuel Cell Sci. Techn.* 1(1) (2004) 2-9.
16. K.L. Chopra, Thin Film Phenomena, McGraw Hill Book Co., New York, 1969.
17. N. Aukland, A. Boudina, D.S. Eddy, J.V. Mantese, M.P. Thompson, S.S. Wang, *J. Mater. Res.* 19(6) (2004) 1723-1729.
18. S.-J. Lee, C.-H. Huang, Y.-P. Chen, *J. Mater. Process Techn.* 140(1-3) 2003 688-693.
19. H. Wang, M.P. Brady, G. Teeter, J.A. Turner, *J. Power Sources* 138(1-2) (2004) 86-93.
20. H. Wang H, M.P. Brady, K.L. More, H.M. Meyer, J.A. Turner, *J. Power Sources* 138(1-2) 2004 86-93.
21. Y. Wang, D.O. Northwood, *J. Power Sources* 191 (2009) 483-488.
22. H. Tawfik, Y. Hung, D. Mahajan, *J. Power Sources* 163(2) (2007) 755-767.